Cross-layer Monitoring in Transparent Optical Networks

Yvan Pointurier, *Member, IEEE,* Mark Coates, *Senior Member, IEEE,* and Michael Rabbat, *Member, IEEE*

***Abstract*—In transparent optical networks, signals propagate over all-optical lightpaths. The absence of regenerating devices that act in the electrical domain renders end-to-end monitoring difficult. Quality of Transmissions (QoT) metrics quantify the degradation in quality that a signal experiences as it traverses a lightpath. Hardware monitors that can directly measure QoT are expensive, which motivates the development of monitoring schemes that require fewer monitors but can still generate accurate QoT estimates. In this paper we describe a monitoring scheme that estimates the QoT of multiple lightpaths in a network. Our focus is on estimating Bit-Error-Rates (BERs), but the methodology is also applicable for other metrics. One of the primary innovations in this monitoring framework is the establishment of "active lightpaths" — lightpaths that carry no useful data but are instead used as measurement probes. We describe a method for choosing where to establish the active lightpaths in order to maximize the information gain. We demonstrate with simulations the possibility to trade-off the amount of costly hardware monitoring equipment with cheaper, temporary active lightpaths, while still achieving accurate monitoring.**

***Index Terms*—Optical networks; monitoring; physical impairments; estimation.**

I. Introduction

Optical signals sustain impairments stemming from their propagation in the fiber medium. In transparent optical networks, the absence of electrical regeneration at every node means that signals can traverse very long distances leading to the accumulation of significant impairments. This can result in the unacceptable degradation of end-to-end transmission performance, as measured by Quality of Transmission (QoT) metrics. A standard QoT metric is the Bit-Error Rate (BER); the Q-factor (defined in Section 2) is another common metric. In transparent optical networks, network operators are interested in monitoring the QoT of each *lightpath*, which is the combination of a route and a wavelength used to transmit a signal. Inadequate performance of a lightpath in terms of BER can indicate that a component on the lightpath is not performing as originally planned (a case of soft failure, where connectivity is maintained but degraded) or that the Routing and Wavelength Assignment algorithm used to pick the degraded lightpath made a poor decision. Signal monitoring is essential, both for the detection of failures and to make better network decisions in order to satisfy service level agreements. It is a challenging task, however, because the absence of electrical generation and the high cost of monitoring devices mean that signals can be monitored only at selected — and possibly few — locations in the network.

In this paper, we describe a QoT monitoring scheme that strives to reduce the amount of hardware needed to perform monitoring while preserving the accuracy of the performance metric estimates. There are two main novel components of this scheme: (i) an optical network probing technique, which we call *active lightpath monitoring*; and (ii) an inference technique that exploits topological knowledge and incorporates regularization to permit performance metric estimation for unmeasured lightpaths.

The active lightpath monitoring technique involves the construction of *lightpath probes*. These are additional lightpaths that are lit only for QoT monitoring purposes; they do not carry any meaningful data (they should carry random bits). They are established for a small period of time (a fraction of a second or a few seconds, depending on the monitored parameters) to make measurements, and the resources they are using can be re-allocated at any time. If in-band probing is undesirable, an out-of-band optical monitoring channel can be used instead.

Automated optical networks employ wavelength-selective switches and reconfigurable optical add/drop multiplexer nodes (so-called "ROADMs"), making it possible to dynamically establish and reconfigure lightpaths. Moreover, such networks must be over-provisioned — at any point in time resources, including transmitters, receivers, and wavelengths, must be ready to accommodate future demands. These resources are natural candidates for use by the active probing framework introduced in this paper since, although they will already be configured and lit, they will not carry customer traffic.

Our proposed inference methodology exploits the spatial correlation between the QoT metrics of all established lightpaths, both the data-carrying lightpaths (we will call these the *passive lightpaths*) and the lightpath probes (*active lightpaths*). This spatial correlation is induced because the physical impairments are caused at the link level, so that if two lightpaths (on different wavelengths) share one or more links, their BERs become correlated. It is only possible to directly monitor a lightpath's performance if it terminates where a hardware monitor is located. This can mean that only a small fraction of the passive (data-carrying) lightpaths are directly measured. The lightpath probes, which are designed to terminate at hardware monitors, provide valuable information (through the correlation) about the performance of the passive lightpaths that cannot be measured.

Manuscript received November 23, 2010. This work is an extended version of a paper presented at ICTON'2008 [1]. This work was supported by the Natural Sciences and Engineering Research Council (NSERC) of Canada through through grant SPSC 356934-2007 and the Mathematics of Information Technology and Complex Systems (MITACS) Network of Centres of Excellence (NCE). This work of Y. Pointurier was conducted while he was with McGill University. He is now with Alcatel–Lucent, Bell Labs, France (corresponding author; e-mail: yvan@ieee.org). M. Coates and M. Rabbat are with the Department of Electrical and Computer Engineering, McGill University, Montréal, Québec, Canada (e-mail: {mark.coates,michael.rabbat}@mcgill.ca).

There is a clear trade-off between the amount of monitoring hardware and the accuracy of QoT estimates. Our monitoring scheme adds another factor into this trade-off — the number of lightpath probes. Our proposed monitoring scheme can preserve the estimation accuracy while reducing the number of hardware monitors by creating lightpath probes. This is an example of "cross-layer" network monitoring, because network layer information (the routing and wavelength assignment state of the network) is exploited to address a physical layer task (lightpath QoT monitoring).

A. Applications

We now highlight a few potential applications of the proposed monitoring framework :

Application 1: users of a core network infrastructure expect that the QoT of their lightpaths is guaranteed to be above a certain level as defined in a Service Level Agreement (SLA) between customer and operator. Enforcing the SLA requires that the core network operator should be able to monitor the QoT of all lightpaths at all times. An operator can use the framework outlined in this work to reduce the amount of monitoring equipment required to achieve this task.

Application 2: Hard failures such as link cuts can be detected and located relatively easily using power monitors, which are deployed in most networking equipment. In contrast, soft failures are caused by the degradation rather than the complete failure of a transmission device. By correlating the alarms generated by the proposed monitoring scheme when monitored quantities become unacceptable, it is possible to detect where a soft failure has occurred using failure localization algorithms such as those in [2], [3]. In a more preventive context, operators can use the proposed monitoring framework to anticipate soft failures.

Application 3: Instead of monitoring the lightpaths that are already established, a network manager may want to predict the QoT of a potential lightpath, before deciding whether to actually establish it. Using monitoring information from lightpaths already established and the estimation framework presented here, QoT prediction before establishment becomes possible (see [4] for one approach).

B. Related Work

There has been a significant amount of work directly addressing the problem of monitoring in transparent optical networks [5]. Typically, in optical networks, monitoring encompasses both *impairment monitoring*, where the focus is a single (type of) impairment (e.g., noise/OSNR or chromatic dispersion) [6], and *performance monitoring*, where the effects of all impairments are evaluated as a whole using a metric that reflects the end-to-end QoT of a lightpath (e.g., BER or Q-factor) [5]. Although we focus in this paper on performance monitoring, the monitoring technique described herein can also be applied to impairment monitoring. Research in this direction has been presented in [4], [7].

The monitoring framework we propose is distinct from existing strategies because it addresses the network-wide estimation of end-to-end (lightpath-level) QoT performance metrics and it involves the establishment of active lightpath probes. There have been other efforts to exploit spatial and temporal correlation in order to perform network-wide path-level performance estimation [8]–[11]. These techniques focus primarily on network performance metrics such as path delay and loss rather than the physical layer QoT metrics. The monitoring framework we propose builds upon the *passive* monitoring scheme (without any active probing) for transparent optical networks that we presented in [11]. As indicated by the simulation results presented in Section IV, the use of active lightpath monitoring makes a major difference in terms of the number of monitoring devices required to achieve a specified estimation accuracy. We presented a preliminary method and associated results in [1].

C. Contributions and Organization

The contributions of this paper are three-fold. First, we adapt estimation techniques to the problem of network-wide monitoring of transparent optical networks, refining them to take advantage of prior knowledge about the physical layer. This allows performance estimation for lightpaths that are not directly measured; the regularization procedure we employ leads to significantly more accurate estimates. Second, we propose the procedure of establishing active lightpaths (lightpath probes) to gain additional information and we provide an algorithm for selecting the routes. The algorithm strives to select the most informative paths to maximize the effective coverage of an existing monitoring hardware deployment. Third, we propose an algorithm for monitor placement to address the scenario when network designers must make decisions about where to deploy equipment to maximize estimation coverage and performance. We present simulation results that indicate that the proposed monitoring scheme provides much better estimates and monitoring coverage than the passive monitoring approach of [11]. The simulations also clearly illustrate the trade-offs between number of monitors, number of lightpath probes, and estimation accuracy.

This paper is organized as follows. In Section II, we state our assumptions concerning the network physical layer and hardware monitors. Section III gives an overview of the estimators used in in this work and presents our active monitoring scheme. We present simulation results in Section IV and we conclude the paper in Section V.

II. Modeling

Our key assumptions are that the physical-layer metrics of interest are (i) measurable by a hardware device; and (ii) approximately linear, in the sense that the end-to-end (path-level) metric associated with a lightpath is approximately equal to the sum, over the traversed links, of the corresponding link-level metrics. We will provide more details and strive to justify these assumptions, but first we outline the physical-layer properties of the networks under study. We assume that transparent optical regeneration, except for standard optical amplification, is not available. We further assume that wavelength converters are not available and that the wavelength continuity constraint holds: lightpaths are established over the same wavelength

from end to end. The latter assumption is not essential (our monitoring framework could readily be adapted to scenarios where it does not hold), but it serves to make our analysis concrete. We also assume that a routing and wavelength assignment (RWA) algorithm is in charge of selecting lightpaths on call arrivals. This algorithm enforces both the wavelength continuity constraint and the QoT constraint. The monitoring technique described in this paper makes no assumption about the nature of the RWA algorithm.

The impairments we consider are amplifier noise and intersymbol interference (ISI). We estimate the BER of a lightpath through its so-called Q-factor: $Q = \frac{\mu_0-\mu_1}{\sigma_0+\sigma_1}$ (where μ_0 and μ_1 are the means of the distributions of the "0" and "1" symbols at the photo-detection stage, and σ_0 and σ_1 are their respective standard deviations). The BER is related to the Q-factor as follows: $\mathrm{BER} = \frac{1}{2}\mathrm{erfc}\big(\mathrm{Q}/\sqrt{2}\big)$. We model the impact of amplifier noise and ISI as additive variances (σ_n^2 and σ_{isi}^2, respectively) in σ_1^2 such that $\sigma_1^2 = \sigma_n^2 + \sigma_{isi}^2$ [12]. In addition, we model single channel nonlinear effects, namely, the interaction between Self-Phase Modulation (SPM) and chromatic dispersion. We ignore other nonlinear effects such as Cross-Phase Modulation (XPM) and Four-Wave Mixing (FWM)[1]. In general, the methods presented in this paper can be used to monitor impairments that either do not depend on the wavelength or have a weak dependence—i.e., impairments that are flat across the transmission spectrum.

We make no assumption about the exact nature of the hardware monitors deployed in the network, but we do require that they can measure electrical power and noise, either directly or indirectly. The hardware monitors can then determine estimates of μ_0, μ_1, σ_0 and σ_1. This type of monitoring falls under the category of histogram-based performance monitoring [13]. We model a hardware monitor as a device located at the extremity of a link, after photo-detection and inside the receiver modules (the alternative of placing a monitor directly on a transmission line requires the undesirable diversion of signal power). A consequence is that we can only measure lightpaths that terminate at a link where a monitor is located. However, our monitoring framework would change only moderately if power diversion were available. Using the notation introduced in the next section, the availability of intermediate measurement points for already established lightpaths can easily be incorporated as additional rows in the monitoring matrix G_m; regarding active lightpaths, the proposed framework can easily be adapted by reinterpreting the number n_a of active lightpaths that can be established in the network as the number of additional monitoring resources used to perform active monitoring.

Although the current work is applied specifically to intensity-modulated networks, it could be generalized to coherent systems, which are currently being deployed in very high capacity backbones. The detection algorithm in coherent receivers (such as DP-QPSK receivers) tracks many physical parameters of lightpaths, such as polarization mode dispersion (PMD), the nonlinear phase, and the chromatic dispersion of the signals, which are responsible for various impairments. In networks where some lightpaths are intensity-modulated (e.g., 10 Gb/s on-off keying) and others are coherent (e.g., 40 Gb/s or 100 Gb/s DP-QPSK), monitoring data available from the coherent receivers terminating established or active lightpaths can be used to estimate the QoT of lightpaths terminated at non-coherent receivers using the estimation framework proposed here and the QoT estimator presented in [14]. In networks equipped with coherent devices only, the coherent receivers can be used in lieu of additional hardware monitors, and the monitoring framework presented in this work can also be leveraged, in conjunction with a QoT estimator adapted to coherent systems.

[1]In existing networks (and envisioned optical networks of the future), the network generally operates in a fully-loaded steady state. Although all wavelengths are not constantly lit, they are all consistently used. In this case, XPM and FWM effects depend only on network topology, in which case they can also be addressed using the framework described in this paper. It is possible that unused wavelengths remain consistently dark, making XPM and FWM effects state- and wavelength-dependent; such dependencies are much more difficult to handle and are out of the scope of this paper.

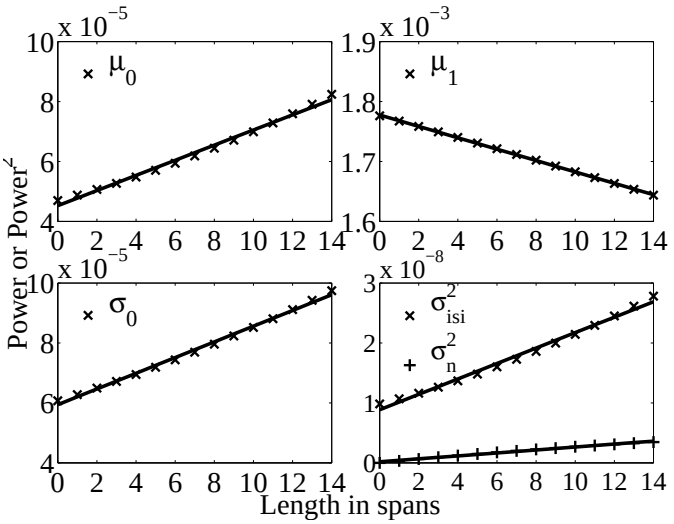

Fig. 1. Linearity of the physical impairments metrics. The depicted metrics are generated using analytical models with the network parameters specified in Section IV. The metrics μ_0, μ_1, σ_0, and $\sigma_{1,isi}$ are generated via propagation simulation using the split-step Fourier method; the metric $\sigma_{1,isi}$ is generated by ASE noise analytical modeling as described in [15]. The solid curves were obtained through linear regression.

III. Active monitoring framework

The active monitoring technique consists of two components. First, we select the set of active lightpaths, and then we estimate the BERs of the unobserved lightpaths using both passive and active measurements. In Section III-A, we describe our inference methodology. In Section III-B, we present the active monitoring technique that establishes additional monitoring lightpaths to improve estimation accuracy. In Section III-C, we propose a hardware monitor placement algorithm.

A. Estimation methodology

We adapt two distinct estimation techniques to the problem at hand: the network kriging procedure of [8] and least-squares minimization with ℓ_2-norm regularization. The latter technique was formerly employed for more general network performance

metric estimation in [9]. Both estimation techniques rely on the assumption of a linear relationship between link-level metrics and the path-level metrics. In transparent optical networks, neither BERs nor Q-factors are linear with respect to the number of spans over which a signal is transmitted, and the required linear relationship does not hold. However, the linearity assumption holds, to within an acceptable approximation error, for each of the four quantities μ_0, μ_1, σ_0, and σ_1^2, as indicated by the linear fits in Fig. 1. We can thus apply these link-level estimation strategies for each of these four quantities and combine the estimates to form an estimate of BER (note that we in fact form estimates of $\log(\mathrm{BER})$, which is a more meaningful QoT metric for network operators).

Consider a transparent optical network of n_ℓ links and N nodes where n_p lightpaths are established. We denote by $\mathbf{y}_p \in \mathbb{R}^{n_p}$ a column vector containing path-level QoT metrics (μ_0, μ_1, σ_0, or σ_1^2 for some lightpaths) and by $\mathbf{x} \in \mathbb{R}^{n_\ell}$ the corresponding link-level metrics. Denote by G_p the routing matrix that describes the network state, that is, $G_p \in \{0,1\}^{n_p \times n_\ell}$, where $(G_p)_{i,j} = 1$ when lightpath i traverses link j. We partition $\mathbf{y}$ and G_p into two components. For the n_m lightpaths that terminate at one of the hardware monitor locations, we denote by $\mathbf{y}_m$ and $G_m \in \{0,1\}^{n_m \times n_\ell}$ the observed (directly measured) path metrics and corresponding routing matrix. For the other unobserved lightpaths, those that do not terminate at a hardware monitor location, we use the notation $\mathbf{y}_n$ and $G_n \in \{0,1\}^{(n_p - n_m) \times n_\ell}$. Thus we have $\mathbf{y}_m = G_m\mathbf{x}$ and $\mathbf{y}_n = G_n\mathbf{x}$.

We also establish a limited number n_a of lightpath probes (active lightpaths) which terminate at nodes with hardware monitors. We defer the discussion of how to choose the routes of these paths until Section III-B. Denote by $G_a \in \{0,1\}^{n_a \times n_\ell}$ the routing matrix of the active lightpaths. Let $\mathbf{y}_a = G_a\mathbf{x}$ be the column vector for metrics corresponding to these active lightpaths. Call $G_A = \left[G_m^T, G_a^T\right]^T$ (where ^{T} denotes transpose) the routing matrix corresponding to all observed lightpaths and $\mathbf{y}_A = \left[\mathbf{y}_m^T, \mathbf{y}_a^T\right]^T$ the column vector containing the metrics for all observed paths. The general estimation problem can be expressed as: given a routing matrix $G_p = [G_m^T, G_n^T]^T$, the end-to-end observations $\mathbf{y}_A = G_A\mathbf{x}$ where the link-level metrics $\mathbf{x}$ are unknown, estimate all unobserved end-to-end metrics $\mathbf{y}_n = G_n\mathbf{x}$.

Denote the estimator $\hat{\mathbf{y}}_n$. If we employ mean-squared error $E[||\hat{\mathbf{y}}_n - \mathbf{y}_n||_2^2]$ as the quality of the estimator, then the best estimator is given by the conditional expectation $E[\mathbf{y}_n|\mathbf{y}_A]$. This cannot be computed unless we have knowledge of the joint distributional structure of $\mathbf{y}_n$ and $\mathbf{y}_A$. We can make the task of finding a good estimator more tractable by focusing on linear estimators (where the estimator can be expressed in the form $\mathbf{B}\mathbf{y}_A$ for some matrix $\mathbf{B}$). Deriving an expression for the best linear estimator does not require knowledge of the joint distribution of $\mathbf{y}_n$ and $\mathbf{y}_A$, but it does require knowledge of the mean and covariance of $\mathbf{x}$. A natural solution is to estimate this mean from the available data, using for example generalized least squares. If enough data is available then the covariance matrix could also be estimated, but we assume a diagonal covariance matrix for simplicity. This leads to the following estimator:

$$\hat{\mathbf{y}}_n = G_n G_A^T (G_A G_A^T)^+ \mathbf{y}_A. \tag{1}$$

Here $(\cdot)^+$ denotes a pseudo-inverse such as the Moore-Penrose inverse. A more general version of this estimator is presented in a paper called "network kriging" [8], and we will retain that name here. The complexity of the kriging estimator is dominated by the complexity of computing the pseudo-inverse in (1), that is, $O((n_m + n_a)^3)$.

The main problem with the network kriging estimator is that there is no positivity constraint (we know that the four metrics of interest are always positive quantities). This can be remedied by projecting onto the viable space of solutions or by incorporating the non-negativity constraint directly in the optimization. In formulating the second estimator, we add the constraint, but we also choose to incorporate an additional prior belief about the "best" explanation for the observed data.[2] The second estimator we formulate in this paper is based on ℓ_2-norm minimization. The associated optimization problem is:

$$\min_{\mathbf{x},\mathbf{r}} \|\mathbf{r}\|_2^2 + \|\mathbf{x}\|_2^2 \tag{2}$$
$$\text{subject to } G_A\mathbf{x} + D_2\mathbf{r} = \mathbf{y}_A, \mathbf{x} \geq 0.$$

In (2), $\mathbf{r}$ is a regularization parameter and D_2 is a diagonal matrix specifying the error tolerance (how closely the path-level metric estimates must match the associated measurements). Problem (2) can be written as a convex quadratic program. Indeed, define vector $\mathbf{z} = [\mathbf{r}^T, \mathbf{x}^T]^T$; then the objective function in (2) is simply $\mathbf{z}^T I \mathbf{z} = \mathbf{z}^T\mathbf{z}$, where all constraints are linear in $\mathbf{z}$. Note that, in general, quadratic programs have objective functions of the form $\mathbf{z}^T G\mathbf{z} + \mathbf{z}^T\mathbf{c}$, with linear constraints on $\mathbf{z}$. In (2), we have $\mathbf{c} = 0$, and the problem is convex since $G = I$ is positive definite. In that case, there are polynomial-time algorithms for solving (2) as well. In particular, there exist efficient solved software packages such as PDCO [16] that can solve problem (2).

The assumption of the (approximate) linear relationships $\mathbf{y}_m = G_m\mathbf{x}$, $\mathbf{y}_n = G_n\mathbf{x}$ and $\mathbf{y}_a = G_a\mathbf{x}$ allows us to use the network kriging and ℓ_2-norm minimization procedures to estimate $\mathbf{y}_n$ given G_n, G_m, G_a and $\mathbf{y}_m$. This estimation procedure is run in turn for $\mathbf{y}_m, \mathbf{y}_n, \mathbf{y}_a \in \{\mu_0, \mu_1, \sigma_0, \sigma_1^2\}$ to return estimates for each of these four quantities for the unobserved lightpaths. Based on these, we can construct estimates for the Q-factors and BERs. Since the four metrics μ_0, μ_1, σ_0, and σ_1^2 are only approximately linear with respect to distance, additional estimation error will accrue from the linearity approximation.

B. Active monitoring

In this section, we address the task of choosing which lightpaths to activate for monitoring. We assume that hardware

[2]Note that the pseudo-inverse in the network kriging estimator does select one of (infinitely) many possible values of $\mathbf{x}$ that can explain the observed data. Thus in employing the kriging estimator we are implicitly specifying a definition of the "best" explanation. In our second estimator, "best" is defined in terms of an attribute of $\hat{\mathbf{x}}$ (minimum ℓ_2-norm). In the kriging estimator, "best" is specified by the choice of the linear mapping function, $G_A^T(G_A G_A^T)^+$ that takes us from $\mathbf{y}_A$ to $\hat{\mathbf{x}}$.

monitors have been placed at fixed locations and that we have a limited budget of n_a active lightpaths. The task is to design an active routing matrix $G_a \in \{0,1\}^{n_a \times n_\ell}$, where each row corresponds to an active lightpath.

Our goal is to choose a set of active paths G_a in order to maximize the "energy" of the unobserved, passive lightpaths (described by G_n) captured by the measurements; this is equivalent to selecting paths to measure (i.e., rows of G_a) that span the space of G_p not captured by G_m and are as linearly independent from G_m as possible. We justify this criterion by recalling that the mean-squared error $E(\|\hat{\mathbf{y}}_n - \mathbf{y}_n\|_2^2)$ of our estimator can be rewritten as the sum of a bias-squared term, $\|E(\hat{\mathbf{y}}_n) - \mathbf{y}_n\|^2$, and a variance term, $E(\|\hat{\mathbf{y}}_n - E(\hat{\mathbf{y}}_n)\|_2^2)$. If we accept the fact that the bias-squared term is difficult to address directly, because it is largely due to our incomplete knowledge about the statistics (e.g., mean and covariance) of the metrics $\mathbf{y}_n$, then it makes sense to minimize the variance term. The variance term increases for each row of G_n that lies outside the row-space of G_A (which we denote by $\mathcal{R}_{G_A}$). Let B_{G_p,G_A} denote a matrix whose columns form an orthonormal basis for the subspace $\mathcal{R}_{G_p} \cup \mathcal{R}_{G_A}$ of unmeasured lightpaths spanned by rows of G_A. Maximizing the energy of the unobserved lightpaths is equivalent to maximizing $\|G_n B_{G_p,G_A}\|_F$, where $\|\cdot\|_F$ denotes the Frobenius norm.

The choice of which active lightpaths to use in forming G_a is subject to the constraints that (i) each row of G_a must correspond to a lightpath that meets the wavelength continuity constraint and (ii) the last link of each active lightpath must be equipped with a monitor. The QoT constraint does not apply for these lightpaths since they do not carry useful data. However, since additional lightpaths use resources and may disturb existing lightpaths through, for example, crosstalk injection, it is desirable to limit the total length of the active lightpaths.

Our active lightpath selection scheme begins by identifying a set of candidate lightpaths that are likely to be good choices. We assume that we can activate lightpaths from any source node to one of the nodes equipped with a monitor. A sensible candidate set could include all of the one-hop and two-hop paths to each monitor, since these paths are short and potentially provide information about multiple paths. One could continue to three-hop and greater neighborhoods of each monitor, but the size of this candidate set would quickly explode. In addition to one-hop and two-hop lightpaths, any active lightpath whose performance is highly correlated with one or more unobserved lighpaths can be very informative. We can construct such lightpaths by appending to each unobserved lightpath the shortest path from its destination to a monitor. Let G_c denote the 0/1-valued matrix whose rows correspond to all of the candidate paths identified; that is we assume that G_c has $n_c > n_a$ rows and exactly n_ℓ columns.

Once we have identified the set of candidate lightpaths, the problem becomes choosing n_a of these candidates with the goal of maximizing $||G_n B_{G_p,G_A}||_F$. The procedure commences by initializing $G_A = G_m$. We then employ a greedy heuristic to select rows from G_c to add to G_A. At each step of the heuristic, we evaluate, for each candidate row i of G_c, a basis $B^{(i)}_{G_p,G_A}$ that would result if we added the row to G_A. We then calculate $||G_n B^{(i)}_{G_p,G_A}||_F$ and choose the row i that maximizes this quantity, adding it to G_A and removing it from G_c. The process is repeated until we have added n_a lightpaths from G_c.

C. Physical monitor placement

When the number of monitors is limited, the monitoring performance can vary substantially depending on where the monitors are located. Estimation performance is improved if more lightpaths terminate at monitors and if the observed lightpaths provide substantial information about the unobserved lightpaths (if they are highly correlated). Optimizing monitor placement requires the ability to accurately predict which lightpaths will be established. This in turn requires that the traffic demands are highly predictable and that a fixed routing and wavelength assignment (RWA) strategy is employed.

In a dynamic transparent optical network, neither of these conditions are likely to hold. But even coarse approximations to the routes and traffic demands can provide us with enough information to choose a set of monitor locations that will be more informative, on average, than a randomly selected set.

We now describe a greedy heuristic for choosing monitor locations. Most RWA algorithms choose shortest paths where possible, so lightpath routes determined by shortest path routing provide a reasonable approximation to the true, possibly time-varying routes. Let the binary matrix G_s denote the shortest path routes in the network for all possible source-destination pairs. If the following algorithm is applied directly to G_s, then we are assuming uniform traffic demand. If we have more knowledge about traffic demands, we can incorporate it by weighting each row in G_s by the demand of the corresponding path.

Our task is to select M monitor locations to maximize estimation performance. This is a similar problem to the active lightpath selection task, except that each monitor location adds the ability to measure multiple lightpaths. We can employ the same algorithm as before, with a minor modification. We initialize G_m as an empty matrix. At each step of the heuristic, we evaluate, for each candidate monitor location i, the rowspace $\mathcal{R}^{(i)}_{G_m}$ (and a corresponding orthonormal basis $B^{(i)}_{G_m}$) that would result if we added to G_m all of the lightpaths that terminate on link i. We then choose the monitor location i that maximizes $||G_s B^{(i)}_{G_m}||_F$. The algorithm terminates when we have selected M monitor locations.

IV. Simulations

We simulate the operation of a scaled-down version of the NSFNET topology (Fig. 2) with standard physical parameters (10 Gbps NRZ signals traveling over 70 km spans of 100% post-dispersion compensated SMF, noise figure of 6 dB, 8 wavelengths); The topology has a diameter close to 800 km, ensuring that end-to-end transparency is feasible even without FEC and with standard, non-advanced dispersion maps and modulation formats. Although the actual physical reach of signals with no regeneration in real networks can be much longer than 800 km thanks for instance to the utilization of FEC, advanced dispersion maps and modulation formats, our

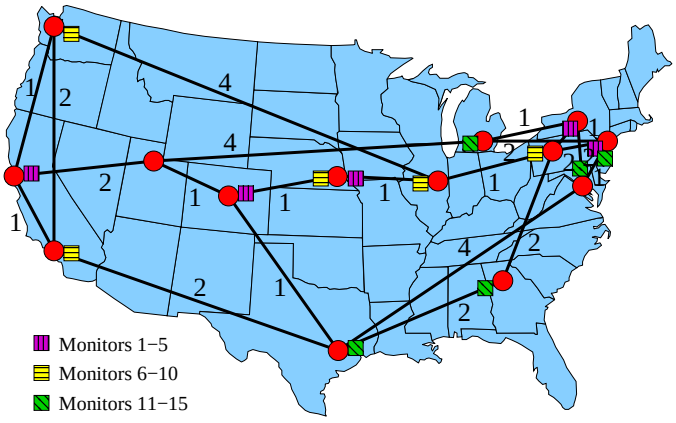

Fig. 2. Network topology used throughout this work. The numbers on the links indicate the number of 70 km spans on each link; the topology we used here is roughly 5 times smaller than the actual NSF network to ensure end-to-end transparency, while retaining topological realism. The squares above link terminations indicate the placement of a monitor when the placement procedure oulined in Section III-C is used.

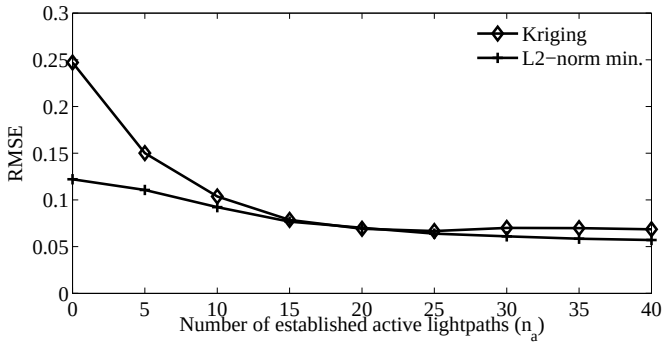

Fig. 3. Relative mean squared error performance of kriging estimator and ℓ_2-norm minimization estimator for a fixed number of hardware monitors (ten), and a varying number of active lightpaths. The case of 0 active lightpaths corresponds to passive monitoring. The kriging estimator generates negative estimates; these are set to zero when calculating estimation error.

models do not depend on those parameters. Only the details but not the essence of the conclusions would change. The network contains 42 unidirectional links and hence would require 42 monitors to gather a complete observation set about the QoT in the network.

Arriving traffic demands are drawn from a uniform distribution over all (source,destination) pairs. Demands are assumed to arrive according to a Poisson process with rate λ and demand durations are exponentially distributed with mean $1/\mu$; numerical results are given for a network load of $\lambda/\mu = 50$ Erlang, which is a usual load for a network of this size. Note, however, that the techniques demonstrated in this paper do not depend on the demand arrival/duration processes.

The route taken by a new demand is determined by an adaptive route-wavelength assignment (RWA) algorithm. The selected route depends on the network state at the time a demand arrives; routes are not necessarily shortest paths, and two demands with the same source and destination do not necessarily take the same route. In each network state, the number of concurrent lightpaths in the network is approximately 50 (varying between 40 and 54 due to the randomness in the demand generation). The results presented in this section are averages over 500 network states.

Monitors are deployed at the locations determined by the monitor placement algorithm described in Section III-C. In Fig. 2, we indicate the locations of the top 15 monitors returned by the placement algorithm described in Section III-C. We use different symbols for the top 5 monitors (monitors 1-5), the next 5 monitors (monitors 6-10) and the again the next 5 monitors (monitors 11-15). Note that the proposed placement algorithm returns nested placements: if we run the placement algorithm to select, independently, M and M' locations such that $M < M'$, then the M locations form a subset of the M' locations returned by the placement algorithm. This property is useful in the context of incremental monitoring hardware deployment.

We first examine the accuracy of the estimators in terms of the relative mean squared error (RMSE) for $\log(\mathrm{BER})$. Fig. 3 compares the accuracy of the two estimators presented in Section III-A for a fixed number of monitors (ten), varying the number of active lightpaths in the network. The kriging estimator generates negative estimates for the BER for 5-10 percent of the lightpaths, even when the number of active lightpaths is relatively high, i.e. 30. These are not physically meaningful values, so we map the $\log(\mathrm{BER})$ to zero for these estimates. The accuracies of both estimators improve as more active lightpaths are injected. The estimator based on ℓ_2-norm minimization outperforms the kriging-based estimator when the number of active lightpaths is relatively small (less than 15), but when more lightpath probes are employed the accuracies are comparable. The remainder of our performance analysis focuses on the ℓ_2-norm minimization estimator.

Fig. 4(a) displays how the RMSE for the ℓ_2-norm minimization estimator is affected by changes in both the number of active lightpaths and the number of monitors. Values for $n_a = 0$ active lightpaths denote passive monitoring results. Establishing even a relatively small number of active lightpaths (e.g., 15) results in a sharp decrease in the estimation error, especially when fewer monitoring devices are installed. There exists a trade-off between the number of physical devices and the number of active lightpaths required to achieve a specifed estimation accuracy. For example, to achieve an estimation error of approximately 7%, one can either deploy 20 monitors and use passive monitoring, or deploy 5 monitors and use active monitoring with 25 active lightpaths. Note that this trade-off could be captured by a single cost function combining both estimation accuracy and number of established active lightpaths n_a (for instance, a linear combination of those two metrics). Such a cost function would likely vary depending on the operator, hence, we are not proposing any such cost function but report detailed results for both estimation accuracy and n_a.

The estimation error does not converge to 0 as n_a increases. It exhibits an error floor that decreases as the number of monitors increases. This can be attributed to the approximation error incurred through the linearization step. Indeed, Fig. 4(b) confirms this assessment. It shows the RMSE in the case where all four metrics μ_0, μ_1, σ_0, and σ_1^2 are artificially

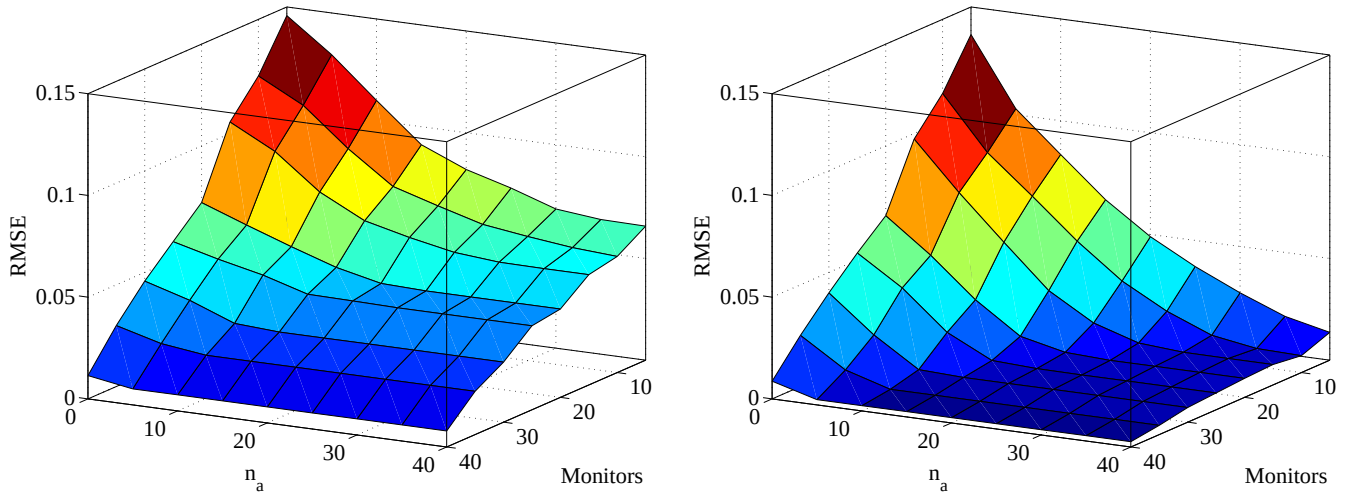

(a) Original metrics.

(b) Linearized metrics

Fig. 4. Relative mean square error for passive (0 active lightpaths) and active monitoring, for various numbers of hardware monitors and active lightpaths. When estimated metrics are artificially linearized, the error floor for large n_a disappears.

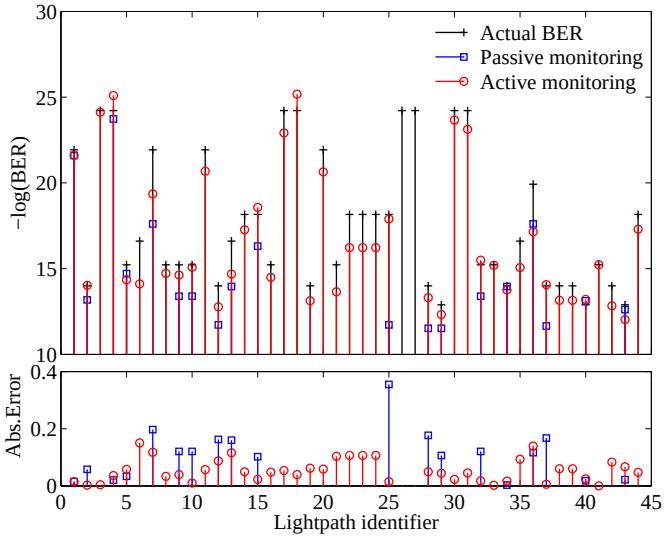

Fig. 5. Sample estimation results for a network configuration with 5 monitors; 9 lightpaths are observed by the monitors, and the BER of 44 lightpaths must be estimated. Estimation results for $-\log(\mathrm{BER})$ are given in the top panel for both passive ($n_a = 0$) and active ($n_a = 20$) monitoring, using the L2-minimization procedure. Missing data points indicate that the estimator failed to return an estimate. In the bottom panel we show the RMSE for both passive and active monitoring.

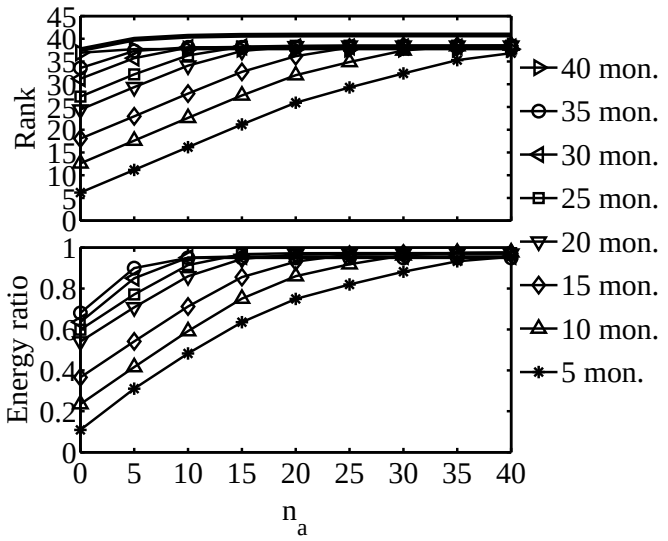

Fig. 6. Top panel: Rank of $\left[G_m^T, G_n^T, G^{*T}_a\right]^T$ (bold) and $\left[G_m^T, G^{*T}_a\right]^T$. The rank of $\left[G_m^T, G^{*T}_a\right]^T$ increases steadily as the number of active lightpaths increases towards the number of links in the network $n_\ell = 42$, indicating that our active lightpaths selection algorithm is adding informative measurements. Bottom panel: The average energy of the unobserved lightpaths that resides in the monitored subspace (the rowspace of $\left[G_m^T, G^{*T}_a\right]^T$) as a function of the number of active lightpaths.

linearized, i.e. they are assigned values that are exactly linear with distance. With genuinely linear metrics, the estimation error converges to 0 as the amount of monitoring hardware or the number of active lightpaths, n_a, increases.

The benefits of active monitoring are illustrated in Fig. 5 using a more concrete example. At the depicted point in time, 53 lightpaths are established in the network and only 9 of these are directly observed by 5 hardware monitors. We show the BER and the absolute error for the 44 unobserved lightpaths (in arbitrary order, labeled from 1 to 44). The plots compare passive monitoring with active monitoring employing $n_a = 20$ active lightpaths. In the case of passive monitoring, the estimation technique cannot generate estimates for 25 lightpaths, whereas with active monitoring, the BERs for only 2 lightpaths are not estimated. The technique cannot generate a meaningful estimate for any lightpath that does not share a link with any of the measured lightpaths. For nearly all lightpaths, the estimates obtained using active monitoring case are consistently closer to the real BER values than the passive monitoring estimates. There is no apparent correlation between the values of the BERs and the associated RMSE.

As discussed in Section III-B, the active monitoring strategy strives to decrease the "variance term" in the estimation error, which involves trying to construct an observation subspace

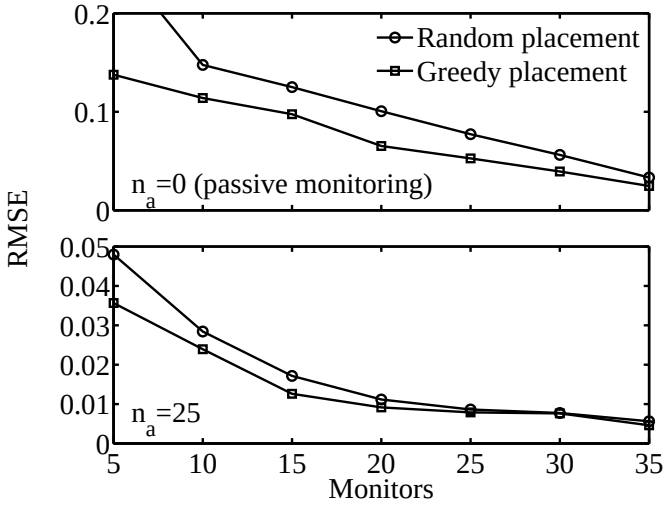

Fig. 7. Impact of the monitor placement algorithm on the estimation accuracy: the RMSE is decreased if the proposed monitor placement algorithm is used (squares) instead of uniform random monitor placement (circles). Results are presented for $n_a = 0$ (passive monitoring; top panel) and $n_a = 25$ active lightpaths (bottom panel). The standard deviation of the error for each configuration is less than 0.01.

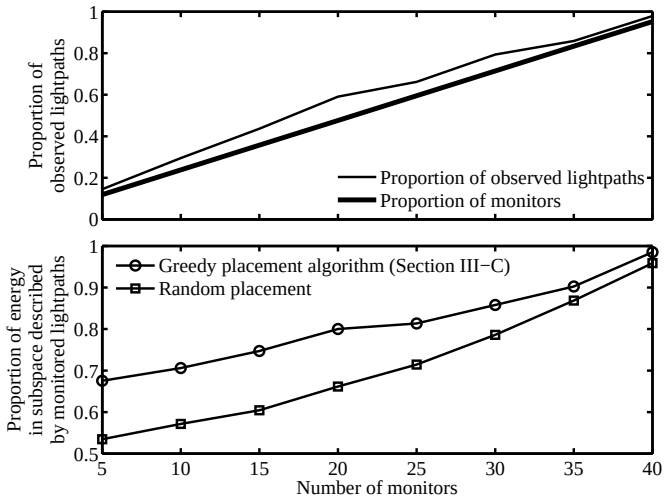

Fig. 8. Top panel: Comparison between the proportion of lightpaths that are observed when the proposed monitor placement scheme is used (thin line) and when random placement is employed (thick line). The random placement line corresponds to the proportion of monitored links out of the total of 42. Bottom panel: The average fraction of energy of the unobserved lightpaths that lies in the monitored subspace, for both the proposed placement scheme and the random placement scheme.

that contains as much of the energy of the unobserved lightpaths as possible. We can measure how successful the algorithm is by assessing the average fraction of energy of each unobserved lightpath that is contained in the constructed space. The rank of the constructed space, $\left[G_m^T, G_a^{*T}\right]^T$, also provides an important indication. If the technique is placing monitors in good locations and activating informative active lightpaths, then the rank should increase rapidly as the number of monitors or active lightpaths is increased (indicating that the addition of resources is providing new information). The top panel of Fig. 6 depicts how the rank of $\left[G_m^T, G_a^{*T}\right]^T$ changes when we vary either the number of monitors or the number of active lightpaths. For low numbers of monitors and active lightpaths, the rank is much less than the number of lit links, making BER estimation inaccurate. However, as n_a increases, $\mathrm{rank}\left(\left[G_m^T, G_a^{*T}\right]^T\right)$ increases with a slope of approximately 1, converging to $\mathrm{rank}\left(\left[G_m^T, G_n^T, G_a^{*T}\right]^T\right)$. This latter value (depicted as a bold line with no markers) is the rank of the complete routing matrix, which includes observed, unobserved and active lightpaths. The bottom panel of Fig. 6 shows the average fraction of energy of the unobserved lightpaths that lies in the space spanned by the vectors $\left[G_m^T, G_a^{*T}\right]^T$. As desired, this fraction increases rapidly as the number of monitors is increased and as the number of active lightpaths is increased.

We now analyze the performance of the monitor placement algorithm, comparing it to a naive strategy of randomly placing monitors in the network. Fig. 7 compares the RMSE achieved by using these two placement strategies followed by application of the ℓ_2-norm minimization estimator. Performance is assessed for the two cases of passive monitoring ($n_a = 0$, top panel) and for 25 active lightpaths ($n_a = 25$, bottom panel), with the number of hardware monitors ranging from 5 to 35. To obtain the random placement curve, we averaged the RMSE for 20 random placements with 50 different network states. The error bars correspond to one standard deviation. The curve corresponding to our proposed monitoring strategy (which is deterministic) is obtained by averaging over 500 network states. The proposed algorithm achieves a 10-20% improvement in estimation accuracy compared to random placement.

The top panel of Fig. 8 displays the proportion n_m/n_p of (passive) lightpaths that are actually observed directly using a monitor when the proposed monitor placement is used. The bold line is the proportion of monitored links (there are 42 links in total). This line also corresponds to the expected fraction of lightpaths that would be observed using a uniform random monitor placement strategy. Using the monitor placement algorithm presented in Section III-C, we monitor more lightpaths (consistently 5-10% more) than would be captured if monitors were randomly placed. Although the number of directly monitored paths has some impact on estimation accuracy, of more interest is how well the monitored lightpaths capture the subspace occupied by the unobserved lightpaths. The bottom panel of Fig. 8 displays the average fraction of energy of the unobserved lightpaths that lies in the monitored subspace, comparing the cases when the proposed placement algorithm is employed to when monitors are placed on random links. It is clear that the greedy placement algorithm results in a monitored subspace that contains much more of the energy of the lightpaths in the network. This leads to the improved estimation performance observed in Fig. 7.

V. Conclusions

We showed that it is possible to decrease the number of hardware monitors needed to monitor the QoT of lightpaths in a transparent optical network by establishing carefully selected "active lightpaths", without sacrificing estimation accuracy. In addition, we studied the sparse monitor placement problem and proposed an algorithm to select locations where hardware monitors should be installed in the network in order to improve estimation accuracy.

The estimation technique relies on a linearization of the quantities involved in the QoT computations. Generalizing our technique to more complex cases where linearity does not hold will be the subject of future work. The estimation technique currently assumes that wavelength-dependent impairments such as XPM and FWM are negligible. It also assumes that the physical layer effects of interest are statistically independent and identically distributed across channels. Accounting for channel dependence is a challenging but important topic of future research.

Acknowledgment

The authors wish to thank the anonymous reviewers for their feedback, which helped improve the manuscript.

Yvan Pointurier (S'02–M'06) received a Diplme d'Ingnieur from Ecole Centrale de Lille, France in 2002, a M.S. in Computer Science in 2002, and a Ph.D. in Electrical Engineering in 2006, both from the University of Virginia, USA. He spent two years at McGill University in Montreal, Canada as a Postdoctoral Fellow and then one year at Athens Information Technology, Greece, as a technical leader for a European Project. In 2009 he joined Alcatel-Lucent Bell Labs, France, as a research engineer. His research interests span design, optimization and monitoring of networks in general, and optical networks in particular.

Dr. Pointurier is a co-recipient of the Best Paper Award at the IEEE ICC 2006 Symposium on Optical Systems and Networks.

Mark J. Coates (M'99–SM'07) received the B.E. degree (first class honors) in computer systems engineering from the University of Adelaide, Australia, in 1995, and the Ph.D. degree in information engineering from the University of Cambridge, U.K., in 1999. He joined McGill University, Montreal, QC, Canada, in 2002, where he is currently an Associate Professor. He was awarded the Texas Instruments Postdoctoral Fellowship in 1999 and was a research associate and lecturer at Rice University, Houston, TX, from 19992001. His research interests include communication and sensor networks, statistical signal processing, and Bayesian and Monte Carlo inference.

Michael G. Rabbat (S'02–M'07) earned the B.Sc. from the University of Illinois at Urbana–Champaign (2001), the M.Sc. degree from Rice University (2003), and the Ph.D. from the University of Wisconsin–Madison (2006), all in electrical engineering. He is currently an Assistant Professor at McGill University. He was a visiting researcher at Applied Signal Technology, Inc., during the summer of 2003. He received the Best Paper Award (Signal Processing and Information Theory Track) at the 2010 IEEE Conference on Distributed Computing in Sensor Systems, Outstanding Student Paper Honorable Mention at the 2006 Conference on Neural Information Processing Systems, the Best Student Paper award at the 2004 ACM/IEEE Conference on Information Processing in Sensor Networks, and the Harold A. Peterson Thesis Prize. His research interests include network monitoring, network inference, and distributed information processing in sensor networks. He is currently an Associate Editor for the ACM Transactions on Sensor Networks.

References

[1] Y. Pointurier, M. Coates, and M. Rabbat, "Active monitoring of all-optical networks," in *Proc. Intl. Conf. Transparent Optical Networks*, Athens, Greece, Jun. 2008.

[2] C. Mas, I. Tomkos, and O. K. Tonguz, "Failure location algorithm for transparent optical networks," *IEEE J. Select. Areas Commun.*, vol. 23, no. 8, pp. 1508–1519, Aug. 2005.

[3] D. C. Kilper, A. Ferguson, B. O. Sullivan, and S. K. Korotky, "Impact of topology and traffic on physical layer monitoring in transparent networks," in *Proc. OSA/IEEE Optical Fiber Comm. Conf.*, San Diego, USA, Mar. 2009.

[4] N. Sambo, Y. Pointurier, F. Cugini, L. Valcarenghi, P. Castoldi, and I. Tomkos, "Lightpath establishment in distributed transparent dynamic optical networks using network kriging," in *Proc. European Conf. Optical Comm.*, Vienna, Austria, Sep. 2009.

[5] D. C. Kilper, R. Bach, D. J. Blumenthal, D. Einstein, T. Landolsi, L. Ostar, M. Preiss, and A. E. Willner, "Optical performance monitoring," *IEEE/OSA J. Lightwave Technol.*, vol. 22, no. 1, pp. 294–304, Jan. 2004.

[6] Dynamic Impairment Constraint Networking for Transparent Mesh Optical Networks (DICONET) Project, "Network impairments in transparent networks and definition of monitoring strategy," DICONET Deliverable D3.1. [Online]. Available: http://www.diconet.eu/

[7] S.-T. Ho and L.-K. Chen, "Monitoring of linearly accumulated optical impairments in all-optical networks," *IEEE/OSA J. Optical Comms. and Networking*, vol. 1, no. 1, pp. 125–141, Jun. 2009.

[8] D. B. Chua, E. D. Kolaczyk, and M. Crovella, "Network kriging," *IEEE J. Select. Areas Commun.*, vol. 24, no. 12, pp. 2263–2272, Dec. 2006.

[9] H. Song, L. Qiu, and Y. Zhang, "NetQuest: A flexible framework for large-scale network measurement," *IEEE/ACM Trans. Networking*, vol. 17, no. 1, pp. 106–119, Feb. 2009.

[10] Y. Chen, D. Bindel, and R. Katz, "Tomography-based overlay network monitoring," in *Proc. ACM SIGCOMM Internet Meas. Conf.*, Karlsruhe, Germany, Aug. 2003.

[11] M. Coates, Y. Pointurier, and M. Rabbat, "Compressed network monitoring for IP and all-optical networks," in *Proc. ACM SIGCOMM Internet Meas. Conf.*, San Diego, USA, Oct. 2007.

[12] Y. Pointurier, M. Brandt-Pearce, T. Deng, and S. Subramaniam, "Fair QoS-aware adaptive Routing and Wavelength Assignment in all-optical networks," in *Proc. IEEE Intl. Conf. Comms.*, Istanbul, Turkey, Jun. 2006.

[13] J. D. Downie and D. J. Tebben, "Performance monitoring of optical networks with synchronous and asynchronous sampling," in *Proc. OSA/IEEE Optical Fiber Comm. Conf.*, Anaheim, USA, Mar. 2001.

[14] F. Cugini, N. Sambo, N. Andriolli, A. Giorgetti, L. Valcarenghi, P. Castoldi, E. L. Rouzic, and J. Poirrier, "Enhancing gmpls signaling protocol for encompassing quality of transmission (qot) in all-optical networks," *IEEE/OSA J. Lightw. Technol.*, vol. 26, no. 19, pp. 3318–3328, Oct. 2008.

[15] G. P. Agrawal, *Fiber-Optic Communications Systems*, 3rd ed. John Wiley & Sons, Inc., 2002.

[16] M. Saunders, "PDCO: Primal-dual interior method for convex objectives," Stanford University, Palo Alto, CA, USA, 2003. [Online]. Available: http://www.stanford.edu/group/SOL/software/pdco.html